Supporting information for the paper:

Effects of surface compliance and relaxation on the frictional properties of lamellar materials
by A. Smolyanitsky, S. Zhu, Z. Deng, T. Li, and R. J. Cannara

Coarse-grained simulation model

We adopt a coarse grained (CG) simulation scheme recently developed by Zhu *et al*. (Ref 23 of main text), which is recapped below and is similar to the model presented in [1]. In the CG scheme, the CG beads are organized in a hexagonal lattice (Fig. S1 (a)) for the simulation of a large sheet of monolayer graphene. The beads are treated as triangular particles, with the normal direction of the triangle perpendicular to the sample surface. The triangle-triangle center distance (CG bead bond length) is 0.568 nm. Effectively one bead represents 16 carbon atoms and an effective area of 0.419 nm^2. The van der Waals (vdW) interaction between two triangular particles is modeled by Lennard-Jones (LJ) interactions. The bonded energy terms consist of a two-body bond energy and three-body angle energy as $U_{bonding}\left(r_{ij},\theta_{ijk}\right)=\sum\frac{1}{2}K_b\left(r_{ij}-r_0\right)^2+\sum\frac{1}{2}K_\theta\left(cos\theta_{ijk}-cos\theta_0\right)^2$, where r_{ij} is the distance between the i^{th} and j^{th} bonded CG beads with r_0 being its corresponding equilibrium distance; θ_{ijk} is the angle between the *i-j* bond and *j-k* bond with $\theta_0 = 120^{\circ}$ being its corresponding equilibrium angle; K_b and K_θ are bond force constant and angle force constant, respectively. The parameterizations of the bond force constant, angle force constant, and vdW parameters are described in detail in Ref. 23 of main text.

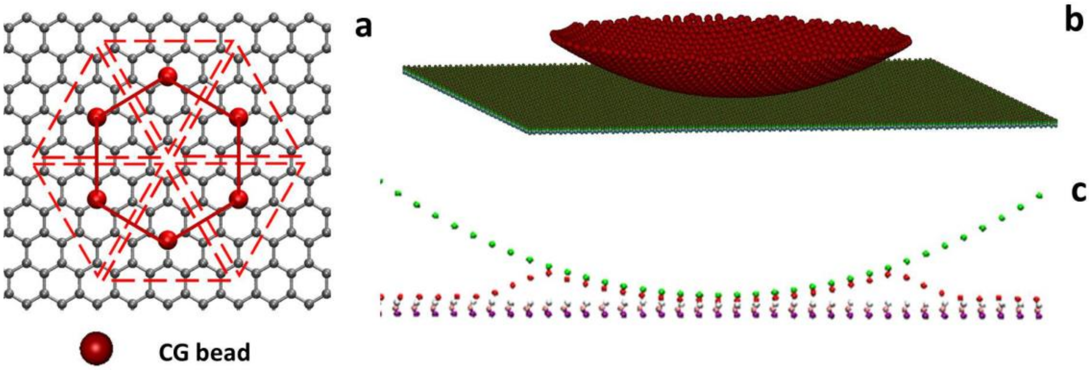

Figure S1. (a) CG interaction scheme (b) CG tip-sample configuration (c) A typical cross-section view of the geometry near the tip for enhanced tip-sample adhesion, where the bottom layer is fixed.

Spectral energy of the measured stick-slip

Because the stick slip process is not truly sinusoidal, a parametric study of δ was performed to ensure a reasonable convergence of $E(k_0)$ values, as shown in Fig. S2. In the main text, we used $\delta = 6.3\ \mathrm{nm}^{-1}$. It is noteworthy that integration of Eq. (2) (main text) from $2\pi/x_{max}$ (the shortest possible wave-vector along a trace of x_{max} length) to a selected large wave-vector value effectively yields the average quadratic variation of $F(x)$ from the entire lateral trace dataset, including all sources of noise. Our calculations over a wide spectral range yielded data qualitatively similar to those obtained with the selected value of δ, as shown in Fig. S2. All results presented in Fig. S2 and Fig. 2 (a) of main text were completely repeatable.

The calculation uncertainty in Eq. (2) of main text arises from the experimental error and, because it evaluates an integral of a quadratic function of the Fourier transform of $F(x)$, the relative uncertainty of calculating $E(k_0)$ is approximately twice the relative measurement error of $F(x)$. For the data presented in Fig. 2 (a) of main text, the average relative error is ≈ 6 %.

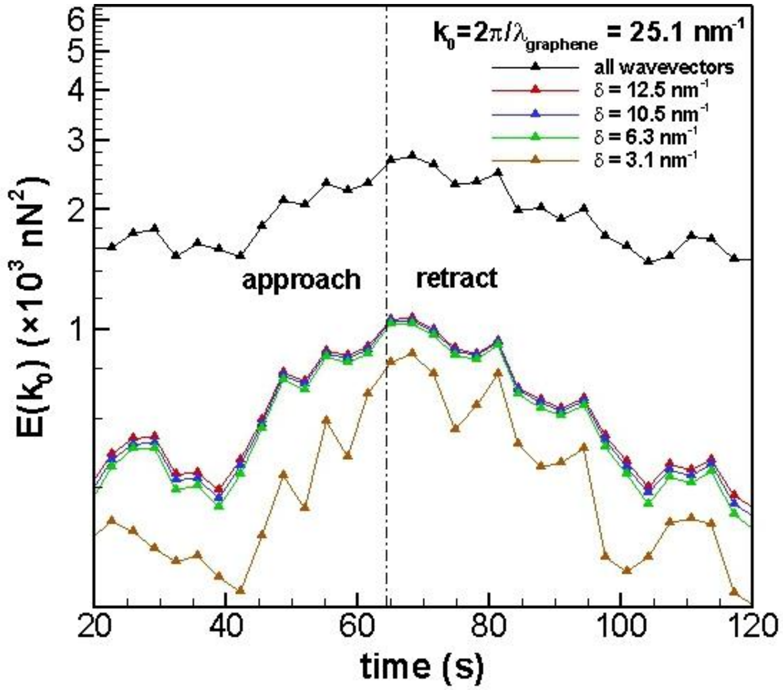

Figure S2. Parametric study of convergence of Eq. (2) (main text) for various values of δ, calculated for a freshly-cleaved graphite data set #1 (main text).

Uncertainty in MD and CG calculations

There is an inherent computational uncertainty associated with the quantities calculated in this work, arising from the choice of interatomic interactions, added thermal noise, as well as from the round-off integration errors. In the worst case, these uncertainties can reach the same order of magnitude as the measured quantities, *e.g.* resulting in systematic scaling of the amplitudes of the lateral force curves in Fig. 3 of main text. However, the qualitative trends within each presented curve, as well as comparisons of trends between the cases considered in the main text remain the same.

Negative friction coefficient on aged MoS_2

Variable-load experiments (similar to those on graphite) were performed on the molybdenum disulfide (MoS_2) surface. The friction-load relationship was obtained by ramping the AFM set point with force feedback on. Fig. S3 shows data acquired on the MoS_2 crystal aged overnight in laboratory air (≈ 25 % relative humidity at 21 °C). To test whether the observed friction-load relationship is reversible, we cycled the load setpoint in the AFM. Fig. S3a plots both raw deflection (blue line) and friction (red circles) signals from the experiment, from which it is apparent that the friction-load curves are reproducible. This is further affirmed by directly plotting friction as a function of load, as shown in Fig. S3b. Figs. S3a and S3b show that friction increases with load during the first tip approach andsubsequently retraces itself with repeated cycling of the load. These data support the notion that a reversible partial exfoliation is occurring also for aged MoS_2. The coefficient of friction (α) is plotted as a function of pull-off force (exposure time) in Fig. S3c, demonstrating that α can be negative after exposure of MoS_2 to laboratory air. We note that the accelerated time frame for the transition to occur, as compared with that observed for graphite, posed a significant challenge to the MoS_2 measurements. Further work to control surface chemistry (transition time), would be required to produce similar data sets for MoS_2 as for graphite, and, for example, compare work of adhesion values with interlayer binding energies.

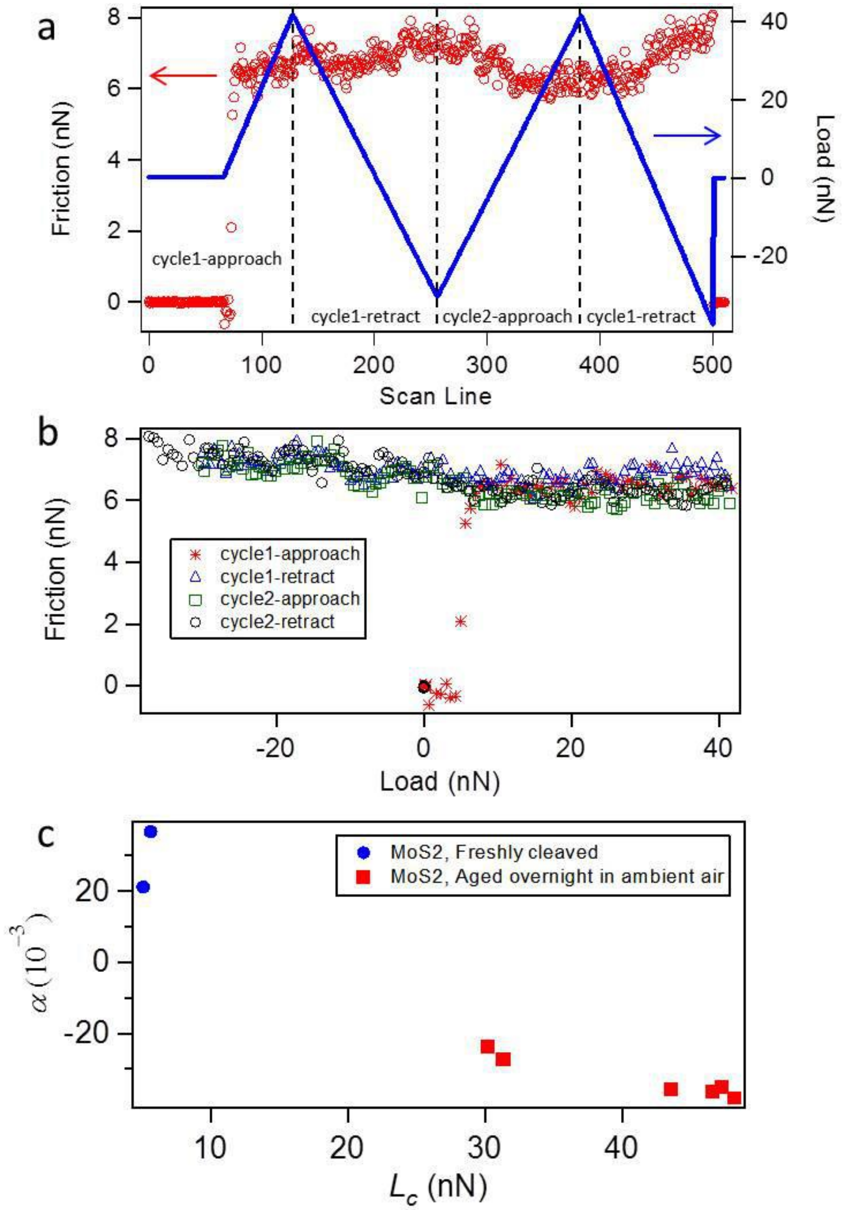

Figure S3. Reversible friction-load curves acquired with the 75 nm-radius ultrananocrystalline diamond probe in [2] on the surface of MoS_2. (a) Friction force and normal load plotted as the function of scanning line (time). (b) The same data in A plotted as a function of load instead of time. (c) Friction coefficient α vs. adhesive force L_C for MoS_2 freshly-cleaved and aged overnight in laboratory air.

1. Kauzlarić, D., et al., *Markovian dissipative coarse grained molecular dynamics for a simple 2D graphene model.* The Journal of Chemical Physics, 2013. **137**(23): p. 234103.
2. Deng, Z., et al., *Adhesion-dependent negative friction coefficient on chemically modified graphite at the nanoscale.* Nature Materials, 2012. **11**(12): p. 1032-1037.